SMOOTH LOCAL PATH PLANNING FOR A MOBILE MANIPULATOR

Carlos Alfaro, M. Isabel Ribeiro, Pedro Lima

Instituto Superior Técnico
Institute for Systems and Robotics
Av. Rovisco Pais 1, 1049-001 Lisboa, Portugal
{calfaro,mir,pal}@isr.ist.utl.pt

Abstract:
This paper presents a path planning technique for a mobile manipulator whose end-effector path is imposed by a given task. The planning is done decoupling the kinematics of the mobile platform and the manipulator, and planning for the former as a normal mobile robot. Two criteria for planning the path were implemented, one minimizing the need to turn the mobile robot and the other minimizing the gravity induced torque components of the manipulator. The linear velocity for following the path is also calculated, as a function of the given end-effector speed. Several results are presented in some typical applications of this planning.

Keywords: Mobile manipulator, Path planning, Nonholonomy, Minimization

1. INTRODUCTION

This paper presents a path planner for a mobile manipulator whose end-effector path is imposed by the task of opening a groove in a wall. By decoupling the kinematics of the mobile platform and that of the manipulator, the planning is performed as for a normal mobile robot, albeit subjected to additional restrictions.

These type of systems have applications in many areas like mining, forestry and construction and are particularly well suited for *human-like* tasks. Opening grooves in walls to install embedded plumbing of several types, such as electricity, water and gas, are common tasks in the construction industry. In general terms, the desired location of the groove is marked by a line painted on the wall, usually at a constant height, and the drilling tool has to be driven along that line.

The paper considers that the drilling tool is carried by a robot arm installed on top of a mobile robot. The aim is to plan a safe path of the mobile manipulator such that the drilling tool follows the line where the groove is to be opened, without considering the opening of the groove itself. No assumption is made on the geometry of the walls where the operation will take place.

A lot of work has been done in this area. The common approaches consider the mobile manipulator as a whole, using the base and manipulator combined kinematics to plan a path, such as in (Papadopoulos and Poulakakis, 2000), (Bayle *et al.*, 2000), (Carriker *et al.*, 1989) and (Carriker *et al.*, 1991), or plan a path coordinating motion and manipulating trough a control algorithm as in (Yamamoto and Yun, 1994). This paper takes a different approach, as it decouples the kinematics of the mobile platform and that of the manipulator. The path planned for the mobile manipulator, subject to the constraint of having the end-effector following the reference path defined by the painted line, is calculated using current

techniques for mobile robots, such as the ones from (Scheuer and Fraichard, 1997), (Graf and Hostalet, 2001), (Laumond *et al.*, 1994), (Fleury *et al.*, 1995), (Nagy and Kelly, 2001) and (Kanayama and Hartman, 1997).

The mobile platform is considered as nonholonomic and the linear and angular velocities are the two degrees of freedom available for platform control and thus, for path following control. This work uses a path planning technique that defines the planned path as a function of its curvature using a measure of smoothness of the path as described in (Kanayama and Hartman, 1997).

To adjust the path to the manipulator task, a set of way-points are defined on the line to follow. Based on these way-points (defined on the walls), a new set of way-points for the mobile platform path are defined, at floor level, according to a specified distance criteria. There is a one to one correspondence between these two sets of way points. The algorithm presented in this paper plans a smooth path of the mobile robot that contains the floor level way-points and that simultaneously guarantees that the end-effector of the manipulator always reaches the line painted on the wall.

We consider the distance between the vertical projection of each wall level way-point and the corresponding floor-level way-point. The set of distances is obtained from the optimization of a given criteria. Tests were conducted with two distinct criteria. The first obtains the minimum turning path leading to a smooth navigation control. The second criteria is related with the manipulator, and aims at minimizing the gravity induced joint torque components. The two criteria lead to different planned paths.

The adopted approach of minimizing a cost to plan the path of a mobile manipulator is similar to the one used in (Bayle *et al.*, 2000), (Carriker *et al.*, 1989) and (Carriker *et al.*, 1991), except that in these references the entire kinematic structure of the mobile manipulator is used while we consider either the mobile robot or the arm kinematics. Cost minimization is implemented using the simulated annealing technique, explained in (Kirkpatrick *et al.*, 1983).

Given the particular characteristics of the application, a desired velocity profile can also be defined. To guarantee the required end-effector speed, the linear velocity of the mobile platform along the planned path has to be evaluated. The algorithm used to calculate these velocity profiles is explained in Section 2.2.

The paper organization is the following: Section 2 describes the mobile manipulator, the definition of the manipulator path, the restrictions to the platform path and the spacial relation between the two paths. Section 3 presents the technique used to generate the mobile platform path, describing the smooth path calculation, the way-point distances selection and the minimizing algorithm implemented. Section 4 presents several planned path results as well as the corresponding linear velocity profiles. Finally, Section 5 presents the conclusions and discusses further work.

2. PATH RESTRICTIONS

The mobile manipulator is composed by a rectangular differential driven mobile platform with a three joint arm mounted on the geometric rotation center of the platform. The arm has one vertical rotation joint and two serial segments forming a two joint planar arm. As the opening of the groove is beyond the scope of this paper, the task is determined as a function of the position of the end effector, regardless of its orientation.

It is considered that the line painted on the wall has a constant given height. The walls are assumed vertical and flat, forming corners, either inward or outward, at their intersections. It is assumed that the position and height of the lines are known, either by the information of a preloaded CAD diagram or using computer vision to extract their location on the walls.

2.1 Restrictions to the platform path

The path followed by the mobile manipulator is restricted by the existing obstacles, either a priori know or unknown. In the present case, the only known obstacles are the walls that the manipulator has to follow. Other unknown dynamic obstacles are not considered in this paper as the objective is to plan an a priori path for the mobile manipulator, that at a latter phase can be changed to accommodate unknown obstacles. For planning purposes, the platform is considered inside of a circle of radius R. Along the path the distance between the platform center of rotation and the closest wall/obstacle should be greater than R, i.e.,

$$\text{distance}(\text{platform}, \text{walls}) > R. \qquad (1)$$

On the other hand, the end-effector has to reach the desired positions along the line painted on the wall, this adding a restriction to the platform path. In the case of a 3 joint arm, this restriction can be expressed as a function of the distance d between the base of the arm and the projection of the desired end-effector position, measured along the plane of the manipulator. Note that this plane is not necessarily orthogonal to the walls.

In Figure 1, the plane of the manipulator is shown, where z is the desired height relative to the base of the arm and d is the distance from the base of

the arm to the wall, evaluated in the plane of the manipulator. The angles θ_2 and θ_3 are the joint values and l_2 and l_3 are the segment lengths. For a given height of the end-effector position, measured from the base of the arm, z, there is a minimum and a maximum value of d that guarantees that the end-effector reaches the wall.
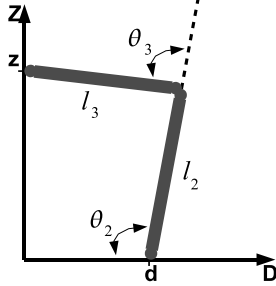

Fig. 1. Plane of the manipulator segments

The referred limits on d can be defined, in general, without imposing limits to the joint values. Rather, they result from the limitations imposed by the length of the segments. From Figure 1 and using the cosines law, the restrictions on d are expressed as

$$
\begin{aligned}
|\cos(\theta_3)| &= \left| \frac{d^2 + z^2 - l_2^2 - l_3^2}{2 l_2 l_3} \right| \leq 1 \\
\Rightarrow & \begin{cases} d \leq \sqrt{(l_2 + l_3)^2 - z^2} \longrightarrow \text{maximum} \\ d \geq \sqrt{(l_2 - l_3)^2 - z^2} \longrightarrow \text{minimum} \end{cases}
\end{aligned} \tag{2}
$$

The limits in (2) are only valid when the arguments of the square-roots are positive. When $(l_2 - l_3)^2 < z^2$, the lower-bound distance limit is set to zero. When $(l_2 + l_3)^2 < z^2$, the wall point is unreachable, because even with the manipulator completely stretched it will not reach the wall. Any path planned for the mobile platform has to satisfy both (1) and (2).

2.2 Relation between manipulator and platform path

When the mobile platform follows the planned path, the manipulator has to follow the path defined by the line on the wall. These two paths are different in geometry and length and so a relation between the positions of the mobile platform and the end-effector for all points of the paths is required. This relation is defined by the position of the mobile platform relative to the start and end points of each segment of the platform path.

Figure 2 represents a inward corner wall profile with the arrows showing the direction in which the painted line has to be followed. The way-points marked on the line, represented by c_1, c_2 and c_3 are points in $\mathcal{R}^3$ with the third component being the desired height. Note that c_2 is at the intersection of two line segments. Let v_{c_1} and v_{c_2} be the required velocities with which each section

of the manipulator path is to be followed. For each c_i a corresponding way-point, defined at floor level, is chosen along the dotted lines represented in the figure. These lines are orthogonal to planar walls or defined along the bisections of corners.
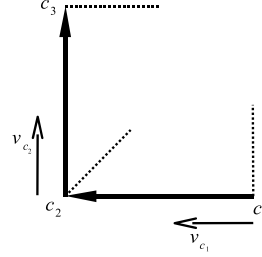

Fig. 2. Manipulator path, with the way-points and section velocities

With this geometry, Figure 3 represents the relationship between the paths of the mobile platform and that of the end-effector. In this figure, X is the current position of the mobile platform along an evaluated path with starting and final positions at X_0 and X_f and c_X is the end-effector position. Note that, at this position, the manipulator plane is not orthogonal to the wall. The distance to the wall, evaluated on the manipulator plane, is d. The orientation of the manipulator plane is only a priori defined at each way-point of the platform path. In between these, i.e., along the platform path, the orientation may change.

Along each segment of the platform path, the vector X is projected orthogonally on the vector v defined by X_0 and X_f. Let the projection be X_p. The ratio between the distance travelled on that line, $\|X_p\|$, and the total distance to travel, $\|v\|$, by the mobile robot is equal to the ratio, equally defined, for the end-effector relative to its path on the wall, i.e.,

$$
\frac{\|X_p\|}{\|v\|} = \frac{v^\top X}{\|v\|^2} = \frac{\|c_X\|}{\|c\|}. \tag{3}
$$

In the above, the vector c is defined by the way-points c_1 and c_2 and c_X is the end-effector position along c when the mobile robot is at X.
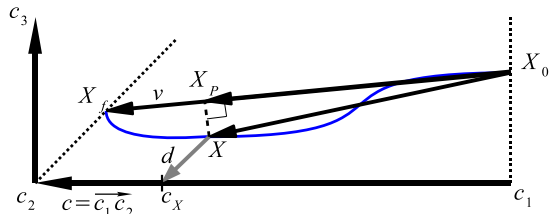

Fig. 3. Relation between platform path position and manipulator path position

From this geometric relation between the paths, a similar relation between the desired speed of the manipulator path and the speed of the platform is derived. Let $s(t)$ be the length of the platform

path followed up to time t and $v_P(t)$ the desired platform linear speed profile. Then,

$$s(t) = \int_0^t v_P(\tau)d\tau. \tag{4}$$

As detailed in Section 3.1, the planned path can be defined by the curvature, $k(s)$, given by the inverse of the turning radius ρ, $k(s) = 1/\rho(s)$ expressed as a function of the path length s. The tangent orientation of the mobile platform along the path is the integral of this curvature, $\theta(s) = \int_0^s k(\tau)d\tau$. Equation (3), can be so rewritten in vectorial form for v and X, the latter being calculated by the integration of the tangent orientation function $\theta(s)$, yielding the new relation in (5). The mobile platform position $X(t)$ is time dependent because, from (4), the followed path length is also time dependent.

$$X(t) = X_t = \left[\int_0^{s(t)} \cos\theta(\tau)d\tau \quad \int_0^{s(t)} \sin\theta(\tau)d\tau\right]^\top$$

$$v = \|v\| \cdot \begin{bmatrix} \cos(\theta_v) \\ \sin(\theta_v) \end{bmatrix} \tag{5}$$

$$c_{X_t} = c_t = \frac{1}{\|v\|}\int_0^{s(t)} \cos(\theta(\tau) - \theta_v)d\tau \cdot c$$

Fixing the desired speed for the end-effector to v_c, c_t can be expressed as,

$$\|c_t\| = d_{c_t} = v_c t$$
$$v_c t = \frac{\|c\|}{\|v\|}\int_0^{s(t)} cos(\theta(\tau) - \theta_v)d\tau. \tag{6}$$

The upper limit of the integral is expressed by (4) that depends of the desired $v_P(t)$. A numerical solution to this equation is obtained by discretizing $s(t)$ and $v_P(t)$, obtaining s_j and v_{P_j} respectively,

$$s(jT) = s_j = \sum_{i=0}^{j} v_P(iT)T \ ; \ v_P(iT) = v_{P_i} \tag{7}$$
$$\delta s_j = s_j - s_{j-1} = v_{P_j}T.$$

Changing (6) with the new discrete length from (7), yields the numerical discrete relation between the discrete approximation of $v_P(t)$ and the manipulator path speed, where $\|c_t\| = v_c t$ is approximated by $\|c_{kT}\| = v_c kT$,

$$v_c kT = \frac{\|c\|}{\|v\|}\sum_{n=0}^{k} \delta s_n \cos(\theta(s_n) - \theta_v). \tag{8}$$

To obtain each of the v_{P_j} from (7), obtaining a numerical discrete approximation to $v_P(t)$, (8) is solved iteratively by rewriting it as a function of all the past know values of v_{P_j},

$$\begin{aligned}
v_c k &= \frac{\|c\|}{\|v\|}\sum_{n=0}^{k} v_{P_n} \cos\left(\theta\left(\sum_{i=0}^{n} v_{P_i}T\right) - \theta_v\right) \\
&= \frac{\|c\|}{\|v\|}\left(\sum_{n=0}^{k-1} v_{P_n} \cos\left(\theta\left(\sum_{i=0}^{n} v_{P_i}T\right) - \theta_v\right)\right. \\
&\quad \left. + v_{P_k} \cos\left(\theta\left(\sum_{i=0}^{k-1} v_{P_i}T + v_{P_k}T\right) - \theta_v\right)\right).
\end{aligned} \tag{9}$$

3. PATH GENERATION

The manipulator path is defined by the wall line to follow, and a series of way-points defined on it. The position of these way-points and the angles between each path segment define the position of the mobile platform way-points, p_i (see Figure 4). These are located at floor-level, either along lines orthogonal to the manipulator path segments or along the bisecting lines between the segments. Their position is determined by the distances, d_i.

The orientation of the mobile platform on each of these way-points is perpendicular to the represented dotted lines, to maintain a pseudo-parallel posture of the mobile manipulator relative to the manipulator path. When the mobile platform is located at the way-points p_i, the plane of the manipulator has a fixed orientation such that it is orthogonal to the walls or defined along the bisecting lines in corners. Each way-point posture p_i is associated with a distance d_i as displayed in Figure 4. The values of d_i are evaluated according to an optimization criteria (see Section 3.2) and satisfy the constraints (1)-(2).

An example of the way-point postures is presented in Figure 4, where an inward corner trajectory line for the manipulator is shown. Distances d_1, d_2 and d_3 indicate the position of the platform way-points on the orthogonal/bisecting lines, and p_1, p_2 and p_3 are the mobile platform postures at each way-point. The planned path is restricted to these way-point postures that act as intermediate start and end points for sections of the complete path.
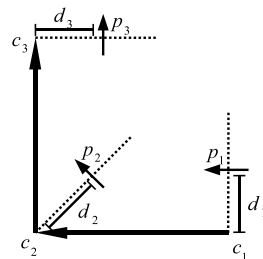

Fig. 4. Example of a inward corner path, the platform way-point postures and their distance to the walls

3.1 Smooth path

Between two consecutive way-points, p_i and p_{i+1}, the smooth path is defined as presented in (Kanayama and Hartman, 1997), where a cost function is used to minimize the centripetal acceleration (or jerk) throughout the path. That reference describes how to calculate the parameters of a quadratic curvature function between two symmetric postures, $p_1 = (x_1, y_1, \theta_1)$ and $p_2 = (x_2, y_2, \theta_2)$ where:

$$\theta_1 - \beta = -(\theta_1 - \beta) \; ; \; \beta = \arctan\left(\frac{y_2 - y_1}{x_2 - x_1}\right). \quad (10)$$

The function $k(s)$ defines the path curvature from p_1 to p_2, and is a continuous function $[-l/2, l/2] \rightarrow \Re$, where l is the positive smooth path length. The tangent orientation function, representing the platform orientation along the path, is given by:

$$\theta(s) = \int_0^s k(\tau)d\tau + \theta_0 \quad -l/2 \le s \le l/2. \quad (11)$$

The generic smooth path point $(x(s), y(s))$ is given by integration of the orientation,

$$\begin{cases} x(s) = \displaystyle\int_0^s \cos\theta(\tau)d\tau + x_0 \\[2mm] y(s) = \displaystyle\int_0^s \sin\theta(\tau)d\tau + y_0. \end{cases} \quad (12)$$

As defined in (Kanayama and Hartman, 1997), a cost function is used to plan the smooth path Π from p_1 to p_2. This function is based on the derivative of the path curvature,

$$\mathrm{cost}(\Pi) = \int_{-l/2}^{l/2} \dot{k}(\tau)^2 d\tau = \int_{-l/2}^{l/2} \ddot{\theta}(\tau)^2 d\tau. \quad (13)$$

If the smooth path Π is followed at a constant linear speed, $\dot{k}(s)$ is equal to the variation of the vehicle centripetal acceleration, also called jerk. Therefore, minimizing this cost function, can be seen as minimizing the complexity of the navigation control. The function $k(s)$ that minimizes (13), for a smooth path with length l, is given by,

$$\begin{aligned} l &= \frac{d}{D(\alpha)} \quad \begin{cases} d = \|p_2 - p_1\| \\ \alpha = \theta_2 - \theta_1 \end{cases} \\ k(s) &= \frac{3}{2}\frac{\alpha D(\alpha)}{d} - \frac{6\alpha D(\alpha)^3}{d^3}s^2 \\ D(\alpha) &= 2\int_0^{1/2} \cos\left(\alpha\left(\frac{3}{2} - 2s^2\right)s\right) ds \end{aligned} \quad (14)$$

When postures p_1 and p_2 do not form a symmetric pair, the referred paper describes a way of finding an intermediate posture. Then, the smooth path between the start and end points is defined by two consecutive local smooth paths. By calculating the local smooth path between each platform path way-point, the entire smooth path is generated.

3.2 Way-point distance selection

The main issue in selecting the way-points p_i is the evaluation of the distances d_i. Two distinct criteria for the choice of d_i were defined, each considering a cost function whose value is defined by the platform path. Regardless of the criteria, all d_i satisfy the constraints (1)-(2).

Considering smoothness alone, any valid path generated by any set of way-points p_i, would suffice for following the manipulator path. However, a path is only considered valid when no point along it violates any of the restrictions, either the distance to the walls, (1), or the distance from the manipulator base to the corresponding point on the manipulator path, (2). The optimization algorithm guarantees that these conditions are fulfilled in a solution. However, there is no formal proof on solution existence.

3.2.1. Minimum turning path This criteria aims at minimizing the orientation variation of the mobile platform, leading to the simplest possible path. This is achieved by maximizing the minimum turning radius of each locally smooth segment of the path. As the turning radius is the inverse of the curvature, $\rho(s) = \frac{1}{k(s)}$, its minimum is obtained when $k(s)$ is maximum. From (14) one can infer that when $s = 0$, $k(0) = \frac{3}{2}\frac{\alpha D(\alpha)}{d}$ is the maximum. The cost function to minimize is then the sum of $k(0)$ for each path segment. As the smooth path segment parameters are dependent on the way-point distances, by selecting the distances that minimize (15), the desired minimum turning path is calculated.

$$\mathrm{cost}_{\text{min. turning}} = \sum \frac{3}{2}\frac{\alpha D(\alpha)}{d}. \quad (15)$$

An example path result for a inward corner line following by the manipulator is shown in Figure 5. It is visible both the smoothness of the turning path and the way the orientation variation is reduced to the minimum possible. The thick line is the line to follow on the wall and the thin line is the limit of the free space for the mobile platform not to hit the walls.

3.2.2. Minimum gravity torque path The second criteria uses the dynamics of the manipulator arm to choose the best values of d_i associated with the way-points p_i. The pose of the manipulator depends on the relation between the platform and the manipulator paths presented in Section 2.2. The cost function is defined as the sum of the average joint torque components throughout the path that depend on the influence of gravity.
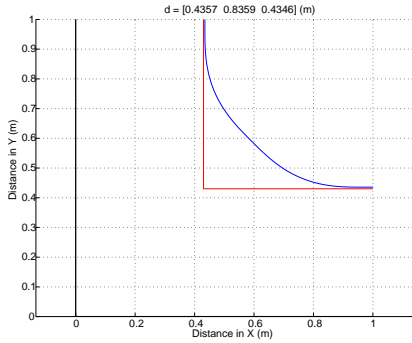
Fig. 5. Example of the minimum turning path for an inward corner

These torque components represent the energy used by the manipulator to move and keep in place as it follows the manipulator path. By minimizing the average gravity torque, the overall expended energy is minimized. On (16) the gravity torque components for the 3 joint arm are expressed, where m_2 and m_3 are the mass of the segments,

$$\begin{cases} \tau_1 = 0 \\ \tau_2 = gm_3l_3c_{23} + gc_2l_2(m_2 + m_3) \\ \tau_3 = gm_3l_3c_{23} \end{cases}$$

$$\sum_{i=1}^{3} \tau_i = 2m_3l_3c_{23} + gc_2l_2(m_2 + m_3). \qquad (16)$$

To evaluate the average gravity torque, the path is discretized and for each point the manipulator pose and the torques are calculated. These are added and divided by the total length of the path. In Figure 6 an example inward corner path result is shown, where is visible that the average distance from the platform path to the manipulator is reduced, relative to the results presented in Figure 5.
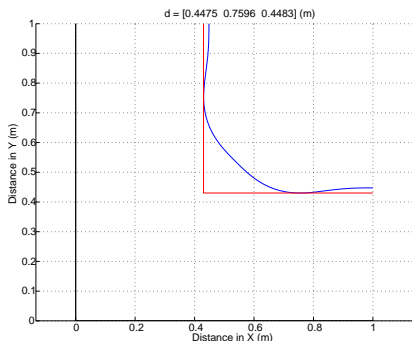

Fig. 6. Example of the minimum gravity torque path for an inward corner

3.3 Cost minimizing algorithm

Given the cost functions just defined, we aim at evaluating the values of d_i associated with each p_i. The two cost functions presented in 3.2.1 and 3.2.2 are very complex, and a closed form of their value as a function of the way-point distances is not easily possible. This leads to the use of numerical methods to find the way-points distances d_i that

lead to the minimum. Several methods were tested such as the cycled coordinate method where the minimum was searched alternately for each d_i, the *Rosenbrock* method and the more complex *Hooke and Jeeves* method. These numerical methods could easily get stuck on local minimums, depending on the initial estimate for the distances, and would never achieve the global minimum.

In light of these results and following the idea suggested in (Carriker *et al.*, 1991) for a similar problem, the simulated annealing technique, presented in (Kirkpatrick *et al.*, 1983), was implemented and used. This technique consists on assigning a *temperature* to the system and starting from a valid initial estimate and its cost. Then the system is passed though a *cooling* processes, where at each step small random variations to the actual estimate are made. If the path generated is a valid one in terms of not violating any restriction, the cost is calculated.

Adding to a normal cost descent search algorithm, not only the new lower cost paths are accepted, but there is also a finite probability that a path with a higher cost than the previous best can be chosen, allowing the escape from local minima. New estimates are generated until an equilibrium is reached at the current temperature, which is then reduced and the process repeated. When the temperature has reduced sufficiently, the technique behaves as a standard descent, as the probability of a higher cost path being accepted is very small, approaching then the local minima.

In addition to the general simulated annealing technique, the best cost path values from each temperature cooling iteration is saved. The next iteration starts either with the latest estimation calculated or with this best cost one, depending on the exponential probability relation between the cost of the two estimates. This change improved greatly the performance of the technique.

4. RESULTS

This section presents simulated results, in some common situations of corners formed by the walls to follow. In Figure 7 an outward corner is followed by the end-effector and the resulting minimum turning path is shown. It is visible the simple curvature of the path, turning the least necessary as desired. Figure 8 represents the correspondent platform linear velocity profile for a constant end-effector speed of $0.005m/s$. The same speed is used for all subsequent examples. As before, the thick line is the line to follow on the wall and the thin line is the limit of the free space for the mobile platform not to hit the walls.

In Figure 9 the same corner is considered but the path yields the minimum manipulator gravity
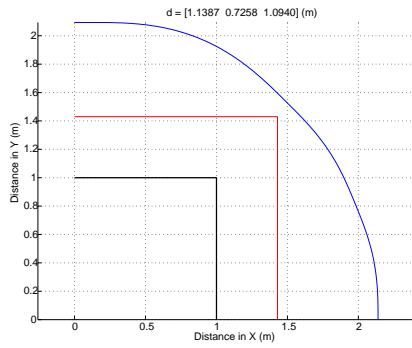
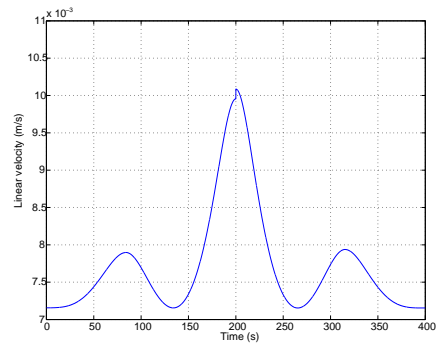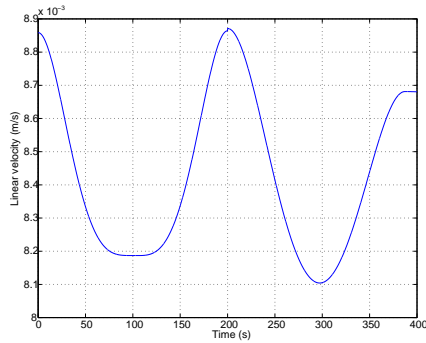Fig. 7. Minimum turning path for an outward corner

Fig. 8. Platform velocity profile for the minimum turning path for an outward corner

torque. The average distance of the platform to the wall is greatly reduced, but the path is more complex adding complexity to the navigation control. Figure 10 displays the linear velocity profile for this path. At the middle of this profile there is a discontinuity, due to the non symmetry of the path and the velocity being calculated separately for each section.
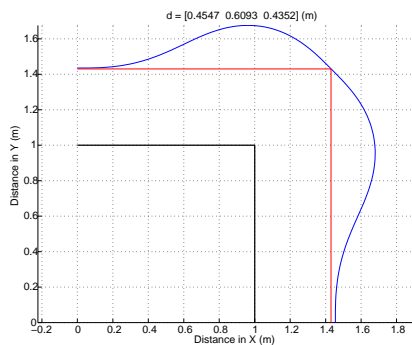

Fig. 9. Minimum gravity torque path for an outward corner

In Figure 11 the minimum turning path for a double corner is represented, showing the combination between the inward and outward corner results. Figure 12 shows the platform linear velocity profile for this path. As before, this profile is not continuous due to the separate velocity calculation on each path section.

In Figure 13 the minimum gravity torque path for a double corner is shown; as before, the mobile

Fig. 10. Platform velocity profile for the minimum gravity torque path for an outward corner
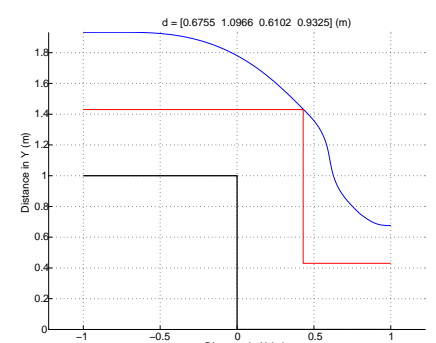

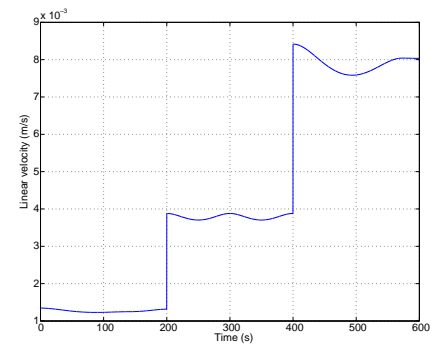Fig. 11. Minimum turning path for two sequential corners

Fig. 12. Platform velocity profile for the minimum turning path for two sequential corners

base maintains a shorter average distance to the wall, although having a section on top that is further away as a result of being a smooth path. Figure 14 shows the linear velocity profile for this path. Once again this profile has discontinuities due to the way it is evaluated.

5. CONCLUSION

In this paper a smooth path generation method for a mobile manipulator based on two distinct criteria was presented. The first criteria generates a minimum curvature path where the mobile platform's orientation variation is minimized. This helps reduce the complexity of the mobile manipulator navigation control. The second criteria uses the dynamics of the manipulator arm, minimizing
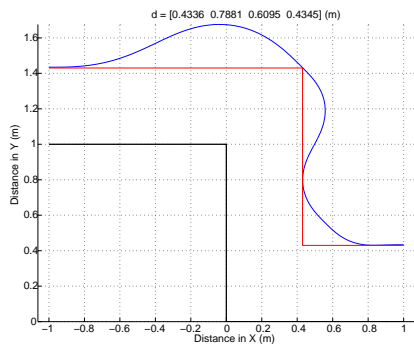
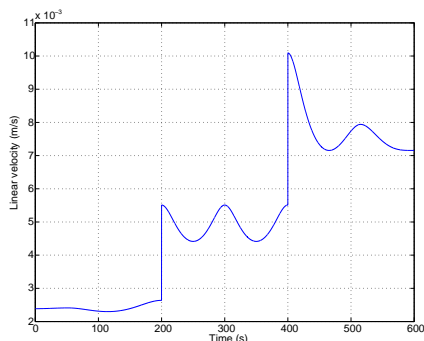Fig. 13. Minimum gravity torque path for two sequential corners

Fig. 14. Platform velocity profile for the minimum gravity torque path for two sequential corners

the average gravity torque components throughout the planned path. Although the resulting platform path is not as simple to navigate as the previous one requiring a more complex control, the energy used overall by the manipulator is greatly reduced.

The simulated annealing minimization algorithm used to find the minimums of the cost functions defined by each criteria, although extensive and time consuming as a search method, yielded very good results in all the situations tested. Where other methods would easily get stuck in local minimums, this algorithm managed to obtain the closest approximation to the global minimums possible.

For each of the planned paths the platform linear velocity profile was obtained, using the numerical relation between the desired end-effector speed and the platform linear speed. The resulting profiles present very smooth characteristics, and in the case of the simple corners a noticeable symmetry. On the more complex manipulator paths, the profiles present discontinuities due to the way they are calculated separately for each path segment between way-points. One important characteristic to point out is the greater smoothness of the velocity profiles from the minimum turning paths in relation to the minimum gravity torque ones, having smaller variations in speed value and lower maximum speeds.

In future work, these path planning techniques can be integrated with a larger task planning architecture, which would use the planned paths as a first desired goal for the mobile platform path, altering them at a later point using information obtained from obstacles in the environment. These alterations could be only small and local or more global, requiring a replanning of the path. In both instances the technique presented in this paper could be re-used. The algorithm to calculate the linear velocity profiles can also be altered to better deal with the speed discontinuities that arise between path segments, calculating the profiles globally for all the path.

6. ACKNOWLEDGMENTS

REFERENCES

Bayle, B., J.-Y. Fourquet and M. Renaud (2000). Generalized path generation for a mobile manipulator. *Current Advances in Mechanical Design and Production VII, Eds. MF.Hassan, SM.Megahed, Pergamon, ISBN 0-08-043711-7* pp. 57–66.

Carriker, W.F., Pradeep Khosla and Bruce Krogh (1989). An approach for coordinating mobility and manipulation. In: *IEEE International Conference on Systems Engineering*. pp. 59–63.

Carriker, W.F., Pradeep Khosla and Bruce Krogh (1991). Path planning for mobile manipulators for multiple task execution. *IEEE Trans. on Robotics and Automation* pp. 403–408.

Fleury, Sara, Philippe Souères, Jean-Paul Laumond and Raja Chatila (1995). Primitives for smoothing mobile robot trajectories. *IEEE Trans. on Robotics and Automation* **11**(3), 441–448.

Graf, B. and J. Hostalet (2001). Flexible path planning for nonholonomic mobile robots. In: *Proc. of Eurobot'01*. pp. 199–206.

Kanayama, Y. and B. Hartman (1997). Smooth local path planning for autonomous vehicles. *International Journal of Robotics Research* **16**(3), 263–284.

Kirkpatrick, S., C. D. Gelatt and M. P. Vecchi (1983). Optimization by simulated annealing. *Science* **220**, **4598**, 671–680.

Laumond, J.-P., P.E. Jacobs., M. Taïx. and R.M. Murray (1994). A motion planner for nonholonomic mobile robots. *IEEE Trans. on Robotics and Automation* **10**(5), 577–593.

Nagy, B. and A. Kelly (2001). Trajectory generation for car-like robots using cubic curvature polynomials. In: *Proc. of the International Conference on Field and Service Robotics (FSR 01)*. Helsinki, Finland.

Papadopoulos, E. and J. Poulakakis (2000). Trajectory planning and control for mobile manipulator systems. In: *Proc. of the 8th IEEE Mediterranean Conference on Control and Automation*. Rio, Greece.

Scheuer, A. and T. Fraichard (1997). Continuous-curvature path planning for car-like vehicles. In: *Proc. of the IEEE-RSJ Int. Conf. on Intelligent Robots and Systems*. Vol. 2. Grenoble, France. pp. 997–1003.

Yamamoto, Y. and X. Yun (1994). Coordinating locomotion and manipulation of a mobile manipulator. *IEEE Trans. on Automatic Control* **39**(6), 1326–1332.